

Overlap of electron shells in β and double- β decays

M. I. Krivoruchenko¹ and K. S. Tyrin²

¹ Institute for Theoretical and Experimental Physics
National Research Center "Kurchatov Institute"
B. Cheremushkinskaya 25 117218 Moscow, Russia

² National Research Center "Kurchatov Institute"
pl. Kurchatova 1 123182 Moscow, Russia

Received: date / Revised version: date

Abstract. The β and double- β decay channels, which are not accompanied by excitation of the electron shells, are suppressed due to the nonorthogonality of the electron wave functions of the parent and daughter atoms. The effect is sensitive to the contribution of the outer electron shells. Since valence electrons participate in chemical bonding and collectivize in metals, the decay rates of the unstable nuclides are modified when they are embedded in a host material. Core electrons are less affected by the environment, and their overlap amplitudes are more stable. The suppression effect is estimated for β^- decay of ^{87}Kr , electron capture in ^{163}Ho , and $2\beta^-$ decays of ^{76}Ge , ^{100}Mo , ^{130}Te , and ^{136}Xe . The overlap amplitude of the electron shells enters the relationship between the half-life of neutrinoless 2β decay and the effective electron neutrino Majorana mass.

PACS. 23.40.-s β decay – 31.00.00 Electronic structure of atoms and molecules: theory

1 Introduction

Neutrinos are likely the most promising particles in the search for new physics beyond the Standard Model. Their electroneutrality and exceptionally low masses raise the question of whether neutrinos are Majorana particles. Majorana neutrinos do not support conservation of the total lepton number. The nonconservation of the total lepton number is sought in the processes of neutrinoless $2\beta^-$ decay, neutrinoless double-electron capture (2EC), and others. In the quark sector of the Standard Model, processes with nonconservation of the baryon number, such as proton decay and neutron-antineutron oscillations, play a similar fundamental role. The conservation laws of the total lepton and baryon numbers are not supported by local gauge symmetries of the Standard Model, and in a more general context, these conservation laws can be violated.

The effective electron neutrino Majorana mass, $m_{\beta\beta}$, can be extracted from the measurement of the half-life of the neutrinoless $2\beta^-$ decay and 2EC in the case that the mechanism leading to these processes is the exchange of a light Majorana neutrino. The amplitudes of the neutrinoless $2\beta^-$ decay and 2EC processes, which are not accompanied by excitation of the electron shells, are proportional to $m_{\beta\beta}$, the nuclear matrix element, the axial-vector coupling constant g_A , and the overlap of the electron wave functions of the parent and daughter atoms. The effective neutrino masses that can potentially be extracted from

the experiment depend on the overlap amplitude of the electron shells.

In this paper, we discuss the overlap effect in decays, accompanied by a change in the electric charge of the nucleus. In the next section, the overlap amplitude of the electron levels with identical quantum numbers and the overlap amplitude of the electron shells are analytically found in a simple nonrelativistic model. The model is then generalized by taking into account shielding of the nuclear charge caused by the inner electrons. The estimates show the dominance of the contribution of the electrons in outer orbits to the overlap amplitude of the electron shells. We also consider the relativistic shell model based on the Dirac equation, in which the effective charge of the nucleus is self-consistently determined using the semi-empirical data on the electron binding energies at individual orbits. There are three possible β decay processes: β^- , β^+ , and electron capture (EC), and four possible double- β decay processes: $2\beta^-$, $2\beta^+$, $\beta^+\text{EC}$, and 2EC. In Sect. 3, numerical results based on the relativistic shell model are presented for β^- decay of ^{87}Kr ; EC in ^{163}Ho , studied in the ECHO experiment in order to determine the absolute scale of neutrino masses [1,2]; $2\beta^-$ decays of ^{76}Ge , ^{130}Te and ^{136}Xe , the neutrinoless mode of which is searched for by the collaborations GERDA [3], CUORE [4], and KamLAND-Zen [5], respectively; and neutrinoless $2\beta^-$ decay of ^{100}Mo , searched for by the collaborations NEMO-3 [6], CUPID-Mo [7], and AMoRE [8]. Finally, we

discuss modification of the total β and 2β decay probabilities caused by the overlap of the electron shells.

2 Overlap amplitude

The β and double- β decays are accompanied by a change in the nuclear charge, Z , by one or two units, respectively. Electrons, which are initially in the stationary states of the parent atom, turn into a superposition of stationary states of the daughter atom. For example, the nonorthogonality of the electron wave functions leads to modification of the energy spectrum of EC in ^{163}Ho [9, 10, 11]. In this section, we estimate the survival probability for the ground state of the electron shells in the β and double- β decays. A similar effect of overlapping wave functions of nucleons in double- β decays is discussed in Ref. [12].

2.1 Analytic approach

The standard separation of variables in the energy eigenfunctions of the nonrelativistic Coulomb problem gives

$$\Psi_{nlm}(\mathbf{r}) = Z^{3/2} R_{nl}(Zr) Y_{lm}(\mathbf{n}), \quad (1)$$

where Z is the charge of the nucleus, n is the principal quantum number, l is the orbital angular momentum, m is its projection, and $Y_{lm}(\mathbf{n})$ is the spherical function. The atomic system of units is used, where the electron mass $m_e = 1$ and the Bohr radius $a_0 = 1/(\alpha m) = 1$. $R_{nl}(Zr)$ satisfies the radial Schrödinger equation. The normalization condition of the radial part takes the form

$$Z^3 \int_0^\infty r^2 dr R_{nl}^2(Zr) = 1. \quad (2)$$

This equation holds for any Z . Differentiating both parts of the equation by Z , we find

$$\int_0^\infty r^3 dr R_{nl}(Zr) R'_{nl}(Zr) = -\frac{3}{2Z^4}. \quad (3)$$

The overlap amplitude of electron levels (OAEL) with the identical quantum numbers for atoms with nuclear charges Z and $Z' = Z + \Delta Z$ can be written as follows:

$$O_{nl} = \int_0^\infty r^2 dr Z^{3/2} R_{nl}(Zr) Z'^{3/2} R_{nl}(Z'r). \quad (4)$$

The overlap amplitude O_{nl} determines the probability of finding the electron in its initial state after the decay. We confine ourselves to the case of $Z \gg 1$, which covers medium-heavy and heavy atoms of the experimental interest. Decomposing the term $Z'^{3/2} R_{nl}(Z'r)$ into a power series of $\Delta Z/Z$ to the second order, one obtains

$$O_{nl} = \int_0^\infty r^2 dr Z^{3/2} R_{nl}(Zr) \times \left(1 + \Delta Z \frac{\partial}{\partial Z} + \frac{1}{2} \Delta Z^2 \frac{\partial^2}{\partial Z^2} + \dots \right) Z^{3/2} R_{nl}(Zr). \quad (5)$$

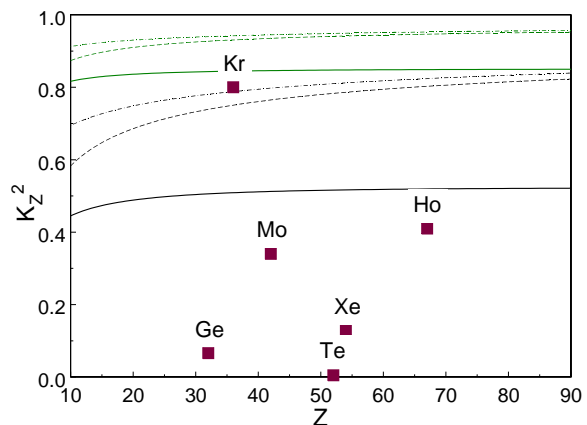


Fig. 1. (color online) Survival probability K_Z^2 of the electron shells as a function of the nuclear charge Z . The green upper curves correspond to the β decay processes with $\Delta Z = \pm 1$. The black lower curves correspond to the double- β decay processes with $\Delta Z = \pm 2$. Dashed and dashed-dotted curves are calculated using Eqs. (10) and (11), respectively. The solid curves are calculated as described in Sect. 2.2. The dark red squares indicate the survival probability $(K_Z^{\text{core shells}})^2$ of core electrons in β^- decay of Kr, electron capture in Ho, and $2\beta^-$ decays of Ge, Mo, Te and Xe, calculated in Sects. 2.3 and 3.

The second-order derivative term can be removed using the radial Schrödinger equation, the normalization condition and Eq. (3). The first-order derivative term vanishes because of condition (3). The first term in parentheses gives the normalization. As a result, we obtain

$$O_{nl} = 1 + \frac{1}{2} \left(-\frac{3}{4} + l(l+1) - 2Z \langle r \rangle + \frac{1}{n^2} Z^2 \langle r^2 \rangle \right) \frac{\Delta Z^2}{Z^2} + \dots,$$

where the average radii are given by (see, e.g., [13])

$$Z \langle r \rangle = \frac{3n^2 - l(l+1)}{2},$$

$$Z^2 \langle r^2 \rangle = n^2 \frac{5n^2 + 1 - 3l(l+1)}{2}.$$

Finally, we obtain

$$O_{nl} = 1 - \frac{1}{8} (1 + 2n^2 - 2l(l+1)) \frac{\Delta Z^2}{Z^2} + \dots \quad (6)$$

The condition $O_{nl}^2 \leq 1$ and the continuity in Z are compatible only with the quadratic dependence in ΔZ and the negative second derivative of O_{nl} .

The OAELs in EC with $_{67}\text{Ho}$ for the states $n = 1, 2, 3$, and 4 and $l = 0$ equal $O_{nl} = 0.999916, 0.999749, 0.999470$, and 0.999081 , whereas relativistic calculations based on the Dirac-Fock code of Ref. [9] yield $0.999910, 0.999716, 0.999389$, and 0.999332 , respectively. The OAELs for $n = 2, 3$, and 4 and $l = 1$ are $O_{nl} = 0.999860, 0.999582$, and

0.999192, whereas Ref. [9] obtains 0.999801, 0.999563, and 0.999524, respectively. The variance in the estimates does not exceed $3 \cdot 10^{-4}$.

We first consider atoms with closed shells. For this case, the following relationship between the nuclear charge and the principal quantum number, n_Z , of the outermost completely filled shell is given by

$$Z = \sum_{n=1}^{n_Z} \sum_{l=0}^{n-1} \sum_{m=-l}^l \sum_{\sigma} 1 = \frac{n_Z(n_Z+1)(2n_Z+1)}{3}, \quad (7)$$

where the summation is carried out over the spin projection $\sigma = \pm 1/2$, the angular momentum projection m , the angular momentum l , and the principal quantum number n .

The overlap amplitude of the electron shells can be found by multiplying the OAELs of all the occupied levels by the principal quantum numbers $\leq n_Z$:

$$K_Z = \prod_{n=1}^{n_Z} \prod_{l=0}^{n-1} \prod_{m=-l}^l \prod_{\sigma} O_{nl}, \quad (8)$$

where the products account for the electron configuration of the electron shells, whereas the shielding of the nucleus by surrounding electrons is neglected. In the EC and 2EC processes, one or two vacancies are formed in the electron shells. Since the O_{nl} are very close to unity, the levels corresponding to these vacancies need not be excluded from (8). The product can be evaluated with the help of the fact that for small ϵ ,

$$\prod_k (1 + c_k \epsilon) \approx \exp\left(\sum_k c_k \epsilon\right), \quad (9)$$

which yields

$$K_Z \approx \exp\left(-\frac{3(n_Z^2 + n_Z + 3)}{40Z} \Delta Z^2\right). \quad (10)$$

Equations (7) - (10) are derived for Z corresponding to integer n_Z . We analytically extend the overlap amplitude to arbitrary Z . In the limit of large Z ,

$$K_Z \approx \exp\left(-\frac{3^{5/3} 2^{1/3}}{80} \frac{\Delta Z^2}{Z^{1/3}}\right). \quad (11)$$

Figure 1 shows K_Z defined by Eqs. (10) and (11) as a function of Z . The approximation of Eq. (10) by Eq. (11) holds with an accuracy better than 3% for $Z \geq 10$ and $\Delta Z = \pm 1$ and better than 10% for $Z \geq 10$ and $\Delta Z = \pm 2$.

Equation (11) implies that EC in ^{163}Ho is not accompanied by excitation of the electron shells with the probability $K_Z^2 \approx 0.95$. In $2\beta^-$ decay of ^{76}Ge , the survival probability equals $K_Z^2 \approx 0.75$.

The neutrinoless double- β decay rate to channels with a low number of holes in the electron shells of the daughter atom is proportional to

$$\Gamma^{0\nu 2\beta} \propto |K_Z m_{\beta\beta} g_A^2 \mathcal{M}^{0\nu 2\beta}|^2, \quad (12)$$

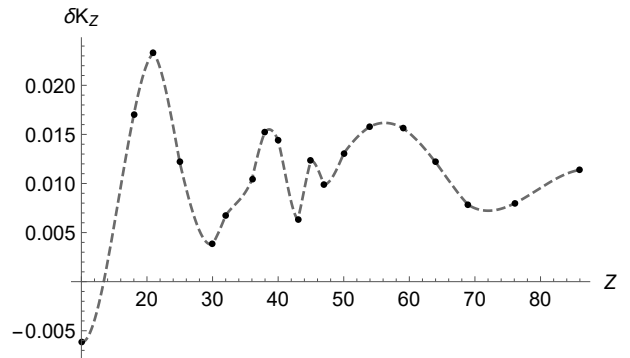


Fig. 2. Accuracy of the $1/Z$ expansion used to derive Eq. (11). The interpolating dashed curve passes through a finite set of values $\delta K_Z = \Delta K_Z / K_Z$ calculated for β decays of atoms with nuclear charge $10 \leq Z \leq 90$.

where $\mathcal{M}^{0\nu 2\beta}$ is the nuclear matrix element. A similar dependence on K_Z exists in the two-neutrino modes of $2\beta^\pm$ decays, $\Gamma^{2\nu 2\beta^\pm} \propto K_Z^2$, and in β decays, $\Gamma^\beta \propto K_Z^2$. The overlap effect suppresses the decay rates and increases the upper limit on the neutrino mass $|m_{\beta\beta}|$, determined from the neutrinoless $2\beta^-$ decay experiments [3, 6, 4, 5].

The accuracy of the $1/Z$ expansion can be tested by comparing the overlap amplitude of the electron shells calculated with the use of the exact OAELs (4) and the exact product (8), on the one hand, and the approximate OAELs (5) and the approximate Eq. (9) used to arrive at Eq. (10) on the other hand. The K_Z of atoms are found by multiplying the OAELs (4) with powers corresponding to the number of electrons on each sub-shell; the result is compared with Eq. (10). The relative errors $\delta K_Z \equiv \Delta K_Z / K_Z$ are plotted in Fig. 2. The accuracy of the $1/Z$ expansion is better than 3% for $Z \geq 10$ and $\Delta Z = \pm 1$.

2.2 Analytic approach with shielding

A more accurate estimate of the overlap amplitude of the electron shells can be obtained by taking into account the shielding of the nucleus charge by electrons. Electrons in an atom move in an effective potential, which can be approximated by the Coulomb potential with an effective charge $Z_{\text{eff}} < Z$. An electron with a principal quantum number n feels an effective charge $Z_{\text{eff}} \approx Z - Z_s$, where Z_s is the number of electrons in the lower orbits with principal quantum numbers $1 \dots n - 1$. Z_s is given by Eq. (7) with n_Z replaced by $n - 1$. Accordingly, in Eq. (6) it is sufficient to make the substitution $Z \rightarrow Z_{\text{eff}}$. The overlap amplitude (8) with the shielding effect taken into account is computed in terms of special functions; however, the final expression is quite cumbersome, so we focus on numerical estimates. The solid curves in Fig. 1 show the total survival probabilities for $\Delta Z = \pm 1$ (upper curves) and ± 2 (lower curves) as functions of the nuclear charge Z ; the estimates (10) and (11) are also shown.

Taking into account shielding, the OAELs in EC with ^{67}Ho for $n = 1, 2, 3$, and 4 and $l = 0$ equal $O_{nl} = 0.999916$,

0.999733, 0.999269, and 0.997287, respectively, while for $n = 2, 3$, and 4 and $l = 1$, the OAELs equal $O_{nl} = 0.999852$, 0.999422, and 0.997616, respectively. The difference from the calculations of Ref. [9] is below 10^{-4} for $n \leq 3$ and $2 \cdot 10^{-3}$ for $n = 4$.

The OAEL of Eq. (6) decreases with increasing n . The partial product over the spin projection, the orbital angular momentum projection, and the orbital momentum yields

$$\prod_{l=0}^{n-1} \prod_{m=-l}^l \prod_{\sigma} O_{nl} \approx \exp\left(-n^2(n^2+2)\frac{\Delta Z^2}{Z^2}\right). \quad (13)$$

The overlap amplitude of the single electron shell with the principal quantum number n is determined by the ratio $\sim n^4/Z^2$. Shielding of the nuclear charge is also important. If Z_{eff} is a screened charge for electrons with principal quantum number n , then the contribution to the overlap amplitude is enhanced as $\sim n^4/Z_{\text{eff}}^2 > n^4/Z^2$. One can show that the error in K_Z associated with the large- Z approximation is below 2% starting from $Z = 10$ for $\Delta Z = \pm 1$.

Equations (6) and (13) show that the maximum contribution to the suppression is given by electrons with high values of n and low values of l . The outermost electron shell contribution is particularly important.

2.3 Relativistic approach

Since the OAELs are close to unity ($O_{nl} - 1 \sim 10^{-2} \div 10^{-4}$), when using software packages for modeling atomic systems, the accuracy of the numerical determination of the electron wave functions should be monitored closely. The use of analytical expressions for electron wave functions has certain advantages in this respect, as analytical methods narrow the range of uncertainties inherent in numerical schemes. A fairly accurate treatment of the overlap effect can be made on the basis of the relativistic Dirac equation in a Coulomb field by determining the effective nuclear charge for each electron level from the known semi-empirical values of the electron binding energies [14]. This approach was used earlier to calculate the Coulomb interaction energy of electron holes for the neutrinoless 2EC problem [15]. Using the known electron binding energies, the effective charges of the parent and daughter nuclei are calculated for each electron level and then substituted into the relativistic energy eigenfunctions of electrons in the Coulomb field. The OAEL

$$O_{njl} = \int_0^\infty r^2 dr [f_{njl}(Z, r)f_{njl}(Z', r) + g_{njl}(Z, r)g_{njl}(Z', r)], \quad (14)$$

with f_{njl} and g_{njl} being the radial functions of bispinor components, is calculated numerically with MAPLE¹ without resorting to a large- Z expansion.

¹ <https://www.maplesoft.com/>

3 Numerical results and discussion

The OAELs (14) for β^- decay of Kr, electron capture in Ho, and $2\beta^-$ decays of Ge, Mo, Te, and Xe are presented in Table 1; the corresponding electron energies and the screened effective nuclear charges are also given.

The estimates presented in Table 1 demonstrate the dominance of contributions of high electron levels and in particular valence electrons. Since valence electrons participate in bonding and collectivize in metals, their effect is the least controlled. A straightforward calculation covering the valence shell contributions yields rather irregular values of the total overlap amplitude K_Z reported in Table 2. The overlap amplitudes of the electron shells in Kr and Xe decays neglect the difference between the solid and vapor-phase systems, for which the electron binding energies are reported in Ref. [14]. The energy of the 5s electron level in Mo is not given in Ref. [14], so this level is not included in K_Z . The effects of electron holes formed in the core shells of the daughter atom in EC or 2EC processes and of missing electrons on the valence shell of the daughter atom in β^- and $2\beta^-$ decays are disregarded because each individual level has only a weak impact on K_Z . Low values of K_Z imply that the decay mode in which electron shells of the daughter atom are unexcited is not dominant. This obviously applies to the decays of germanium and tellurium. To judge which channels dominate in cases with low K_Z , it is necessary to consider transitions to excited states.

The survival probability of core electrons is less affected by the environment. Excluding 4 valence electrons in Ge, we obtain $K_Z^{\text{core shells}} = 0.26$, which should be compared to $K_Z = 6.2 \cdot 10^{-3} \ll K_Z^{\text{core shells}}$. A similar calculation for Kr without 8, Mo without 6, Te without 6, Xe without 8, and Ho without 3 valence electrons yields the values reported in Table 2. To estimate uncertainties in $K_Z^{\text{core shells}}$, it is necessary to perform the calculations using alternative schemes for modeling the electron shell structure. We remark that the outermost subshells of krypton and xenon are filled. Under standard conditions for temperature and pressure, krypton and xenon are inert noble gases that do not usually form chemical bonds with other atoms. The number of valence electrons is, however, the average characteristic of atoms. For example, holmium has a maximum valence of 13, while in chemical compounds, it usually donates three electrons. Krypton usually donates two electrons while forming compounds, etc. The ratio $K_Z/K_Z^{\text{core shells}}$ determines the contribution of the valence shell. The strong inequality $K_Z \ll K_Z^{\text{core shells}}$, which characterizes germanium and tellurium decays, implies that their dominant decay channels are associated with excitations of the valence shells. Given that the overlap amplitude of the electron shells depends on the second power of ΔZ , according to Eq. (11), one can expect similar results for the EC process in ^{81}Kr , discussed in Ref. [17], and 2EC process in ^{124}Xe , which has recently been observed by the XENON Collaboration [18].

The amplitudes of neutrinoless $2\beta^-$ decay and neutrinoless 2EC processes are proportional to the effective

Table 1. Overlap amplitudes O_{njl} of the electron levels with quantum numbers n , j , and l for β^- decay of ^{87}Kr , electron capture in ^{163}Ho , and $2\beta^-$ decays of ^{76}Ge , ^{100}Mo , ^{130}Te , and ^{136}Xe . The electron binding energies ϵ^* from Ref. [14] are given in keV for solid systems referenced to the Fermi level, except for Kr and Xe, where ϵ^* are given for vapor-phase systems referenced to the vacuum level. Z_{eff} is the effective nuclear charge determined from the Dirac equation.

$n2jl$	$\frac{^{32}\text{Ge}}{\epsilon^* Z_{\text{eff}}}$	$\frac{^{34}\text{Se}}{\epsilon^* Z_{\text{eff}}}$	O_{njl}	$\frac{^{36}\text{Kr}}{\epsilon^* Z_{\text{eff}}}$	$\frac{^{37}\text{Rb}}{\epsilon^* Z_{\text{eff}}}$	O_{njl}	$\frac{^{42}\text{Mo}}{\epsilon^* Z_{\text{eff}}}$	$\frac{^{44}\text{Ru}}{\epsilon^* Z_{\text{eff}}}$	O_{njl}
110	11.1031 28.41	12.6578 30.31	0.99832	14.3256 32.21	15.1997 33.17	0.99966	19.9995 37.95	22.1172 39.87	0.99898
210	1.4143 20.32	1.6539 21.96	0.99303	1.9210 23.65	2.0651 24.51	0.99850	2.8655 28.81	3.2240 30.54	0.99599
211	1.2478 19.09	1.4762 20.76	0.99553	1.7272 22.43	1.8639 23.30	0.99908	2.6251 27.60	2.9669 29.31	0.99759
231	1.2167 18.90	1.4358 20.53	0.99570	1.6749 22.17	1.8044 23.01	0.99913	2.5202 27.18	2.8379 28.84	0.99778
310	0.1800 10.90	0.2315 12.36	0.96272	0.2921 13.88	0.3221 14.57	0.99431	0.5046 18.22	0.5850 19.62	0.98696
311	0.1279 9.19	0.1682 10.54	0.96516	0.2218 12.10	0.2474 12.78	0.99439	0.4097 16.43	0.4828 17.83	0.98732
331	0.1208 8.93	0.1619 10.34	0.96031	0.2145 11.90	0.2385 12.55	0.99473	0.3923 16.10	0.4606 17.44	0.98794
332	0.0287 4.36	0.0567 6.12	0.90397	0.0950 7.92	0.1118 8.60	0.99421	0.2303 12.34	0.2836 13.69	0.99055
352	0.0287 4.36	0.0567 6.12	0.90398	0.0938 7.87	0.1103 8.54	0.99427	0.2270 12.25	0.2794 13.59	0.99060
410	0.0050 2.42	0.0120 3.76	0.36980	0.0275 5.68	0.0293 5.87	0.99586	0.0618 8.52	0.0749 9.38	0.96224
411	0.0023 1.64	0.0056 2.57	0.41864	0.0147 4.16	0.0148 4.17	0.99996	0.0348 6.39	0.0431 7.12	0.95900
431				0.0140 4.06	0.0140 4.06	1.00000	0.0348 6.39	0.0431 7.12	0.95902
432							0.0018 1.45	0.0020 1.54	0.99273
452							0.0018 1.45	0.0020 1.54	0.99273
$n2jl$	$\frac{^{52}\text{Te}}{\epsilon^* Z_{\text{eff}}}$	$\frac{^{54}\text{Xe}}{\epsilon^* Z_{\text{eff}}}$	O_{njl}	$\frac{^{54}\text{Xe}}{\epsilon^* Z_{\text{eff}}}$	$\frac{^{56}\text{Ba}}{\epsilon^* Z_{\text{eff}}}$	O_{njl}	$\frac{^{67}\text{Ho}}{\epsilon^* Z_{\text{eff}}}$	$\frac{^{66}\text{Dy}}{\epsilon^* Z_{\text{eff}}}$	O_{njl}
110	31.8138 47.60	34.5644 49.54	0.99928	34.5644 49.54	37.4406 51.49	0.99933	55.6177 62.17	53.7885 61.20	0.99987
210	4.9392 37.65	5.4528 39.51	0.99712	5.4528 39.51	5.9888 41.35	0.99740	9.3942 51.35	9.0458 50.43	0.99956
211	4.6120 36.41	5.1037 38.25	0.99831	5.1037 38.25	5.6236 40.10	0.99845	8.9178 50.09	8.5806 49.17	0.99975
231	4.3414 35.65	4.7822 37.41	0.99852	4.7822 37.41	5.2470 39.17	0.99863	8.0711 48.52	7.7901 47.67	0.99980
310	1.0060 25.68	1.1487 27.43	0.98940	1.1487 27.43	1.2928 29.08	0.99156	2.1283 37.17	2.0468 36.46	0.99906
311	0.8697 23.89	1.0021 25.63	0.99046	1.0021 25.63	1.1367 27.28	0.99243	1.9228 35.36	1.8418 34.62	0.99910
331	0.8187 23.24	0.9406 24.91	0.99095	0.9406 24.91	1.0622 26.47	0.99304	1.7412 33.85	1.6756 33.21	0.99930
332	0.5825 19.61	0.6894 21.33	0.99378	0.6894 21.33	0.7961 22.92	0.99546	1.3915 30.28	1.3325 29.63	0.99959
352	0.5721 19.45	0.6767 21.15	0.99384	0.6767 21.15	0.7807 22.72	0.99553	1.3514 29.88	1.2949 29.25	0.99960
410	0.1683 14.05	0.2133 15.82	0.94280	0.2133 15.82	0.2530 17.22	0.97004	0.4357 22.57	0.4163 22.07	0.99784
411	0.1102 11.38	0.1455 13.07	0.93124	0.1455 13.07	0.1918 15.00	0.93194	0.3435 20.05	0.3318 19.71	0.99890
431	0.1102 11.38	0.1455 13.08	0.93138	0.1455 13.08	0.1797 14.53	0.96003	0.3066 18.97	0.2929 18.55	0.99810
432	0.0398 6.84	0.0695 9.04	0.80895	0.0695 9.04	0.0925 10.43	0.94724	0.1610 13.75	0.1542 13.46	0.99878
452	0.0398 6.84	0.0675 8.91	0.82734	0.0675 8.91	0.0899 10.28	0.94702	0.1610 13.76	0.1542 13.46	0.99878
453							0.0037 2.09	0.0042 2.22	0.99549
473							0.0037 2.09	0.0042 2.22	0.99549
510	0.0116 4.61	0.0234 6.56	0.36726	0.0234 6.56	0.0291 7.31	0.92576	0.0512 9.70	0.0629 10.75	0.93362
511	0.0023 2.06	0.0134 4.96	-0.34644	0.0134 4.96	0.0166 5.52	0.93386	0.0203 6.11	0.0263 6.95	0.90411
531	0.0023 2.06	0.0121 4.71	-0.36107	0.0121 4.72	0.0146 5.18	0.94892	0.0203 6.11	0.0263 6.95	0.90415

electron neutrino Majorana mass

$$m_{\beta\beta} = \sum_i U_{ei}^2 m_i, \quad (15)$$

where $U_{\alpha i}$ is the Pontecorvo–Maki–Nakagawa–Sakata mixing matrix and m_i are the diagonal neutrino masses. The study of cosmic microwave background anisotropies by the Planck Collaboration yields $\sum_i m_i < 0.12$ eV [16].

Exotic interactions beyond the Standard Model can modify the mass of neutrinos in nuclear matter, so the effective electron neutrino Majorana mass observed in $2\beta^-$ decays and 2EC processes may differ from the vacuum value [19]. A similar effect arises from supersymmetric generalizations of the Standard Model [20,21].

The GERDA and KamLAND-Zen collaborations [3,5], from searching the neutrinoless $2\beta^-$ decay with ^{76}Ge and ^{136}Xe , give restrictions on the effective electron neutrino Majorana mass, $|m_{\beta\beta}| < 120 - 260$ meV and $61 - 165$ meV, respectively, by taking into account uncertainties in the nuclear matrix elements and for the unquenched axial-vector coupling $g_A = 1.27$. The constraints $|m_{\beta\beta}| < 330 - 620$ meV and $270 - 760$ meV are obtained by the NEMO-3 and CUORE collaborations [6,4] from searching the neutrinoless $2\beta^-$ decay with ^{100}Mo and ^{130}Te , respectively.

The neutrino mass limits must be supplemented by a new condition, $K_Z = 1$, according to relation (12). The imperfect overlap of the electron shells with moderately low K_Z leads to an increase in the upper limits. For neutrinoless $2\beta^-$ decays of ^{100}Mo and ^{136}Xe , the neutrino mass limits increase by $1/K_Z = 1.8$ and 4.6 times, respectively, and the environment-independent part of the scaling factors equals $1/K_Z^{\text{core shells}} = 1.7$ and 2.8 , respectively.

The low ratios $K_Z/K_Z^{\text{core shells}}$ signal the importance of decay channels with excited valence shells of the daughter atoms. The low values of $K_Z^{\text{core shell}}$ further indicate a noticeable contribution of channels with excited core electrons. The obviously small overlap, $K_Z \ll 1$, observed for the neutrinoless $2\beta^-$ decays of ^{76}Ge and ^{130}Te signifies dominance of decay channels with multiple excited electron shells, which takes us beyond the applicability of relationship (12). In the neutrinoless $2\beta^-$ decays of ^{100}Mo and ^{136}Xe , K_Z and $K_Z^{\text{core shells}}$ deviate from unity only moderately; the probability of such decays obeys relationship (12), which is valid for the daughter atoms with a low number of holes in the electron shells.

The normalized energy spectrum of electron capture in atoms carries information about the electron neutrino mass [1,2]. In Ref. [11], *ab-initio* calculation of excited states up to three electron holes, associated with EC in

Table 2. Total overlap amplitude K_Z and overlap amplitude of core electrons $K_Z^{\text{core shells}}$ in β^- decay of ^{87}Kr , electron capture in ^{163}Ho , and $2\beta^-$ decays of ^{76}Ge , ^{100}Mo , ^{130}Te , and ^{136}Xe . The number of valence electrons of the parent atoms is given in parentheses after the atom symbols. The electron configuration of the parent atoms is shown below the atom symbols.

Overlap amplitude	^{32}Ge (4) [Ar] $3d^{10}4s^24p^2$	^{36}Kr (8) [Ar] $3d^{10}4s^24p^6$	^{42}Mo (6) [Kr] $4d^55s^1$	^{52}Te (6) [Kr] $4d^{10}5s^25p^4$	^{54}Xe (8) [Kr] $4d^{10}5s^25p^6$	^{67}Ho (3) [Xe] $4f^{11}6s^2$
K_Z	$6.2 \cdot 10^{-3}$	0.89	0.56	$1.4 \cdot 10^{-4}$	0.22	0.53
$K_Z^{\text{core shells}}$	0.26	0.90	0.58	0.069	0.36	0.64

^{163}Ho , is performed for transitions with branching ratios above 10^{-3} . We remark that K_Z cancels out from and does not influence the normalized energy spectra of β and double- β decays to channels with a low number of holes in the electron shells of the daughter atoms.

Calorimetric detectors for β and double- β decays measure the total energy released. Suppression of channels with a small number of holes in the electron shells can be compensated by channels associated with multiple excitation of the electron shells of the daughter atoms. Since the binding energy of valence electrons in an atom is approximately 10 eV, to experimentally distinguish the contribution of channels with a small number of holes in the electron shells from the contribution of channels with multiple excitation of the electron shells, it is required to measure the energy of electrons emitted in β^- and $2\beta^-$ decays with a resolution of 10 eV or better. If this strong condition is not satisfied, then the channels in question cannot be distinguished experimentally.

The overlap amplitude of valence shells, $K_Z/K_Z^{\text{core shells}}$, is sensitive to chemical bonds, properties of the environment, etc.; these uncertainties are comparable to the uncertainties inherent in a nuclear structure calculation. Uncertainties in nuclear matrix elements of neutrinoless $2\beta^-$ decay reach 50% (see, e.g., [24]). The axial-vector coupling in nuclei is also quite uncertain; it can be half of its value for a free nucleon [25], which can in turn increase the upper limit of $|m_{\beta\beta}|$ by approximately 4 times. In the case of neutrinoless $2\beta^-$ decay of ^{136}Xe , the valence shell contribution increases the upper limit by $K_Z^{\text{core shells}}/K_Z = 1.6$ times. In the decay of ^{100}Mo , the effect is negligible, while in the decays of ^{76}Ge and ^{130}Te with $K_Z \ll 1$, the valence shell contribution can hardly be quantified with regard to $|m_{\beta\beta}|$ because of the involvement of multiple excited states of electron shells of the daughter atoms.

The experimental limits for neutrinoless 2EC half-lives are weaker compared to neutrinoless $2\beta^-$ decay. One of the best such limits is obtained for the $^{40}\text{Ca} \rightarrow ^{40}\text{Ar}$ decay: $T_{1/2}^{0\nu 2\text{EC}} > 1.4 \cdot 10^{22}$ years [22]. The articular interest in the neutrinoless 2EC is associated with the possibility of resonance enhancement of the decay rate [15, 23]. The valence shell excitations have a strong effect on the K_Z value but are not associated with absorption of a significant amount of energy. The typical binding energy of valence electrons is 10 eV. The resonance condition for the neutrinoless 2EC process is determined by the natural width of the electron levels, which has a similar order of magnitude. Transitions accompanied by the excitations of valence electrons do not strongly violate the resonance condition but can increase K_Z . Holmium atoms used to study the single EC

are embedded in a metallic environment, where the collectivization of valence electrons complicates the estimate of K_Z . The same observation applies to any EC experiments using a substance in a metallic phase.

4 Conclusions

In this paper, the overlap amplitude of electron shells in β and double- β decays was considered. The deviation of OAELs from unity increases with an increase in the principal quantum number and a decrease in the orbital angular momentum. A simple estimate (11) shows that the product of OAELs significantly deviates from unity despite the fact that the values of the OAELs are very close to unity. The total overlap amplitude K_Z is found to be sensitive to the electron configuration of the outer shells. The valence electrons provide a particularly large but irregular contribution to K_Z . Given that valence electrons participate in bonding and collectivize in metals, the phase state of the substance, impurities, and molecular structure of the elements affect the value of K_Z . The overlap amplitude of core electrons, $K_Z^{\text{core shells}}$, is less sensitive to the environment. The relativistic self-consistent scheme described in Sect. 2.3 was used to calculate K_Z and $K_Z^{\text{core shells}}$ for β^- decay of ^{87}Kr , electron capture in ^{163}Ho , and $2\beta^-$ decays of ^{76}Ge , ^{100}Mo , ^{130}Te , and ^{136}Xe . The results show that the overlap effect is numerically significant or highly significant, with $K_Z^{\text{core shells}}$ ranging from 0.90 (Kr) to 0.069 (Te). The overlap amplitude of core electrons provides an upper limit for the total overlap amplitude, which depends on the environment.

In the dominant channels of β and double- β decays, the electron shells of the daughter atoms, as hitherto assumed, remain with a low number of excitations. In transitions of this type, the overlap amplitude K_Z cancels out from the normalized energy spectra and branching ratios, while the total decay rates are suppressed as $\Gamma^{\beta/2\beta} \sim K_Z^2$. Such suppression requires renormalization of the nuclear matrix elements and the axial-vector coupling g_A extracted from β and double- β decay experiments. One can assume that the observed quenching of g_A is partly due to the imperfect overlap of the electron shells.

The molybdenum atom has particularly stable overlap factors in the $2\beta^-$ decay: $K_Z = 0.56$ and $K_Z^{\text{core shells}} = 0.58$. The neutrino mass limits extracted from the experimental searches for neutrinoless $2\beta^-$ decay of ^{100}Mo suffer from only minimal uncertainties related to the overlap of the electron shells. For krypton and xenon, we obtained $K_Z = 0.89$ and $K_Z^{\text{core shells}} = 0.90$ and obtained $K_Z = 0.22$ and $K_Z^{\text{core shells}} = 0.46$, respectively. Since

krypton and xenon have more stable configurations than other elements of the periodic table, their overlap amplitudes are expected to be weakly dependent on the environment. The overlap effect with moderately low K_Z modifies the relationship between $m_{\beta\beta}$ and the neutrinoless 2β decay widths as described by Eq. (12). The overlap amplitudes of ^{76}Ge and ^{130}Te are surprisingly low and sensitive to the contribution of the valence shells. Therefore, the dominant $2\beta^-$ decay channels of ^{76}Ge and ^{130}Te contain daughter atoms with multiple excited electron shells. At $K_Z \ll 1$, the relationship between $m_{\beta\beta}$ and the neutrinoless 2β decay widths is more complex than that in Eq. (12).

The overlap effect is important for fitting phenomenological parameters of nuclear structure models and determination of quantitative relationships between the half-lives of neutrinoless 2β decays and the effective electron neutrino Majorana mass.

The authors are indebted to F. Danevich for the discussion of experimental limitations in the β spectrum measurements. This work is partially supported by RFBR Grant No. 18-02-00733.

References

1. L. Gastaldo, K. Blaum, A. Doerr *et al.*, *The Electron Capture ^{163}Ho Experiment ECHO: an overview*, J. Low Temp. Phys. **176**, 876 (2014).
2. C. Hassel, K. Blaum, T. Day Goodacre *et al.*, *Recent Results for the ECHO Experiment*, J. Low. Temp. Phys. **184**, 910 (2016).
3. M. Agostini *et al.* [GERDA Collaboration], *Improved Limit on Neutrinoless Double- β Decay of ^{76}Ge from GERDA Phase II*, Phys. Rev. Lett. **120**, 132503 (2018).
4. K. Alfonso *et al.* [CUORE Collaboration], *Search for Neutrinoless Double-Beta Decay of ^{130}Te with CUORE-0*, Phys. Rev. Lett. **115**, 102502 (2015).
5. A. Gando *et al.* [KamLAND-Zen Collaboration], *Search for Majorana Neutrinos near the Inverted Mass Hierarchy Region with KamLAND-Zen*, Phys. Rev. Lett. **117**, 082503 (2016) Addendum: [Phys. Rev. Lett. **117**, 109903 (2016)].
6. R. Arnold *et al.* [NEMO-3 Collaboration], *Results of the search for neutrinoless double- β decay in ^{100}Mo with the NEMO-3 experiment*, Phys. Rev. D **92**, 072011 (2015).
7. E. Armengaud *et al.*, *The CUPID-Mo experiment for neutrinoless double-beta decay: performance and prospects*, arXiv:1909.02994 [physics.ins-det].
8. V. Alenkov *et al.*, *First Results from the AMoRE-Pilot neutrinoless double beta decay experiment*, Eur. Phys. J. C **79**, 791 (2019).
9. L. Gastaldo, F. Šimkovic, Amand Faessler, *Electron capture in ^{163}Ho , overlap plus exchange corrections and neutrino mass*, J. Phys. G **42**, 015108 (2015).
10. A. Faessler, L. Gastaldo and F. Šimkovic, *Neutrino Mass, Electron Capture and the Shake-off Contributions*, Phys. Rev. C **95**, 045502 (2017).
11. M. Braß, C. Enss, L. Gastaldo, R. J. Green, and M. W. Haverkort, *Ab initio calculation of the calorimetric electron-capture spectrum of ^{163}Ho : Intra-atomic decay into bound states*, Phys. Rev. C **97**, 054620 (2018).
12. F. Šimkovic, Ch. C. Moustakidis, L. Pacearescu, Amand Faessler, *Proton-neutron pairing in the deformed BCS approach*, Phys. Rev. C **68**, 054319 (2003).
13. L. D. Landau and E. M. Lifschitz, *Quantum Mechanics. Non-relativistic Theory*, 3-rd ed. (Nauka, Moscow, 1974).
14. F. B. Larkins, *Semiempirical Auger-electron energies for elements $10 \leq Z \leq 100$* , At. Data and Nucl. Data Tables **20**, 311 - 387 (1977).
15. M. I. Krivoruchenko, F. Šimkovic, D. Frekers, Amand Faessler, *Resonance enhancement of neutrinoless double electron capture*, Nucl. Phys. A **859**, 140 (2011).
16. N. Aghanim *et al.* (Planck Collaboration), *Planck 2018 results. VI. Cosmological parameters*, arXiv:1807.06209 (2018).
17. S. S. Ratkevich, A. M. Gangapshv, Yu. M. Gavriluk *et al.*, *Comparative study of the double-K-shell-vacancy production in single- and double-electron-capture decay*, Phys. Rev. C **96**, 065502 (2017).
18. E. Aprile *et al.* [XENON Collaboration], *Observation of two-neutrino double electron capture in ^{124}Xe with XENON1T*, Nature **568**, 532 (2019).
19. S. Kovalenko, M. I. Krivoruchenko, F. Šimkovic, *Neutrino propagation in nuclear medium and neutrinoless double- β decay*, Phys. Rev. Lett. **112**, 142503 (2014).
20. R. N. Mohapatra, *New contributions to neutrinoless double-beta decay in supersymmetric theories*, Phys. Rev. D **34**, 3457 (1986).
21. J. D. Vergados, *Neutrinoless double beta-decay without majorana neutrinos in supersymmetric theories*, Phys. Lett. B **184**, 55 (1987).
22. G. Angloher *et al.*, *New limits on double electron capture of ^{40}Ca and ^{180}W* , J. Phys. G **43**, 095202 (2016).
23. S. Eliseev, C. Roux, K. Blaum *et al.*, *Resonant Enhancement of Neutrinoless Double-Electron Capture in Gd-152*, Phys. Rev. Lett. **106**, 052504 (2011).
24. F. Šimkovic, A. Faessler, V. Rodin, P. Vogel and J. Engel, *Anatomy of nuclear matrix elements for neutrinoless double-beta decay*, Phys. Rev. C **77**, 045503 (2008).
25. J. T. Suhonen, *Value of the Axial-Vector Coupling Strength in β and $\beta\beta$ Decays: A Review*, Front. in Phys. **5**, 55 (2017).